Electronic Supplementary Material (ESI) for Materials Chemistry Frontiers.
This journal is © the Partner Organisations 2021

ESI for

Living supramolecular polymerization of an AIE-active Ir(III) complex with irregular emission

Yan Chen, Liyan Zhang, Lei Wang, Lin Guo and Chun Liu*

State Key Laboratory of Fine Chemicals, Dalian University of Technology, Linggong Road 2, Dalian 116024, China. E-mail: cliu@dlut.edu.cn

Contents

Materials and methods *S2-S3*

Synthesis and characterization *S2-S3*

Thermodynamic study *S3*

Single crystal *S3*

Kinetic and thermodynamic study *S4-S7*

The experiments for living supramolecular polymerization *S7-S8*

The experiments for living supramolecular polymerization cycle *S8-S11*

Self-assembly mode *S11-S13*

NMR and HRMS spectra *S14-S15*

Reference *S16*

Materials and methods

Synthetic routes of cyclometalating ligand and Ir(III) complex

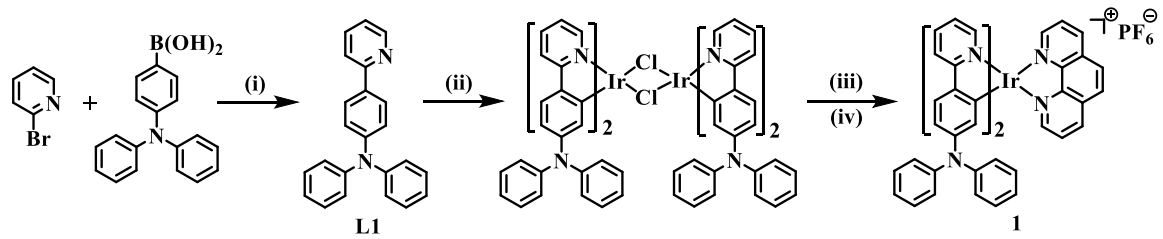

Fig. S1 Synthetic route of **1**. (i) $Pd(OAc)_2$, K_2CO_3, Air, $EtOH/H_2O$, 3:1(v/v), 80 °C, 30 min. (ii) $IrCl_3 \cdot 3H_2O$, $EtOCH_2CH_2OH/H_2O$, 3:1(v/v), 120 °C, N_2, 24 h. (iii) 1,10-phenanthroline, $EtOCH_2CH_2OH$ 12 mL, 120 °C, N_2, 24 h. (iv) KPF_6, RT, 3 h.

Synthetic procedure of ligand L1

A mixture of 2-bromopyridine (1 mmol), 1.5 equiv. of 4-(diphenylamino)phenylboronic acid, 2 equiv. of K_2CO_3, $Pd(OAc)_2$ (1.5 mol%), ethanol/water (3:1 v/v) was stirred at 80 °C in air for the indicated time. The reaction mixture was added to brine (20 mL) and extracted with dichloromethane. The solvent was concentrated under vacuum, and the product was isolated by column chromatography.

Synthetic procedure of Ir(III) complex 1

$IrCl_3 \cdot 3H_2O$ (0.2 mmol) was reacted with 2.5 equiv. of the cyclometalating ligand **L1** in a mixture of 2-ethoxyethanol and water (9 mL/3 mL) at 120 °C under nitrogen for 24 h. Upon cooling to room temperature, the suspension was concentrated under vacuum. The solid was completely dried to give the crude cyclometalated Ir(III) chloride-bridged dimer. Without further purification, the dimeric Ir(III) complex was subsequently reacted with 3 equiv. of 1,10-phenanthroline in 2-ethoxyethanol at 120 °C under nitrogen for 24 h. After cooling to room temperature, a 10-fold excess of saturated KPF_6 solution was added and stirred for 3 h. The reaction mixture was added to water (15 mL) and extracted with dichloromethane. The product was isolated by column chromatography.

Characterization of Ir(III) complex 1

^{1}H NMR (400 MHz, DMSO-d_6): δ 8.89 (dd, J = 8.2, 1.2 Hz, 2H), 8.42 - 8.32 (m, 4H), 8.13 (dd, J = 8.2, 5.1 Hz, 2H), 7.80 (d, J = 8.3 Hz, 2H), 7.72 (d, J = 8.7 Hz, 2H), 7.49 - 7.42 (m, 2H), 7.25 (t, J = 7.9 Hz, 8H), 7.05 (t, J = 7.4 Hz, 6H), 6.98 (d, J = 7.6 Hz, 8H), 6.55 (dd, J = 8.6, 2.3 Hz, 2H), 6.53 - 6.46 (m, 2H), 5.88 (d, J = 2.3 Hz, 2H); ^{13}C NMR (125 MHz, DMSO-d_6): δ 171.49, 156.26, 153.60, 153.25, 151.46, 151.33, 142.86, 141.88, 136.27, 134.64, 133.50, 132.39, 130.96, 130.85, 130.61, 129.06, 127.26, 127.15, 124.15, 124.03, 119.09; HRMS

(MALDI-TOF) *m/z*: $[M - PF_6]^+$ calcd for $C_{58}H_{42}N_6Ir$, 1015.3100; found 1015.3111. $[M - PF_6$ - 1,10-phenanthroline$]^+$ calcd for $C_{46}H_{34}N_4Ir$, 835.2413; found 835.2629.

Thermodynamic study

First, the suspension of **1NP** with f_w of 85% was directly prepared inside a quartz cuvette equipped with a magnetic stirrer (50 μM, 1500 rpm). After the conversion of **1NP** to **1NS** was finished, the solution of monomer **1** in CH_3CN at the same concentration was added to obtain a new suspension at 60% water content according to the depolymerization curve (Fig. 2a). Finally, the above suspension (f_w: 60%, 50 μM) was stirred at 1500 rpm for 10 min to fully assemble the added monomers, and the resulted suspension was used for thermodynamic study.

(1) Heating process: the absorption spectra were recorded with a heating step of 1 K and heating rate of 1 K min^{-1} with 30 seconds of equilibration time.

(2) Cooling process: the above suspension of **1NS** (f_w: 60%, 50 μM) heated up to 343 K and was left at this temperature for 10 min to fully depolymerize **1NS** into monomers. The absorption spectra were recorded with a cooling step of 1 K and cooling rate of 1 K min^{-1} with 30 seconds of equilibration time.

Single crystal

Summary of crystallographic data and details of data collection for complex **1** are given in Supporting Information Tab. S2. Single crystal with suitable dimensions was selected under an optical microscope and mounted onto a glass fiber for data collection. Intensity data for complex **1** were collected on a Bruker SMART APEX diffractometer equipped with a CCD area detector and a Cu-Kα (λ = 1.54178 Å) radiation source at 173.15 K. The data integration and reduction were processed using the SMART and SAINT software.[1,2] The structure was solved by direct methods using SHELXTL and refined on F^2 by the full-matrix least-squares method using the program SHELXL-2017 and Olex2.[3,4] All the non-hydrogen atoms were refined with anisotropic thermal displacement coefficients. Hydrogen atoms were fixed geometrically at calculated positions and allowed to ride on the parent non-hydrogen atoms. The X-ray crystallographic coordinates for the structure of complex **1** have been deposited at the Cambridge Crystallographic Data Centre (CCDC) under deposition number CCDC 1952377. These data can be obtained free of charge from the Cambridge Crystallographic Data Centre via www.ccdc.cam.ac.uk/data_request/cif.

Kinetic and thermodynamic study

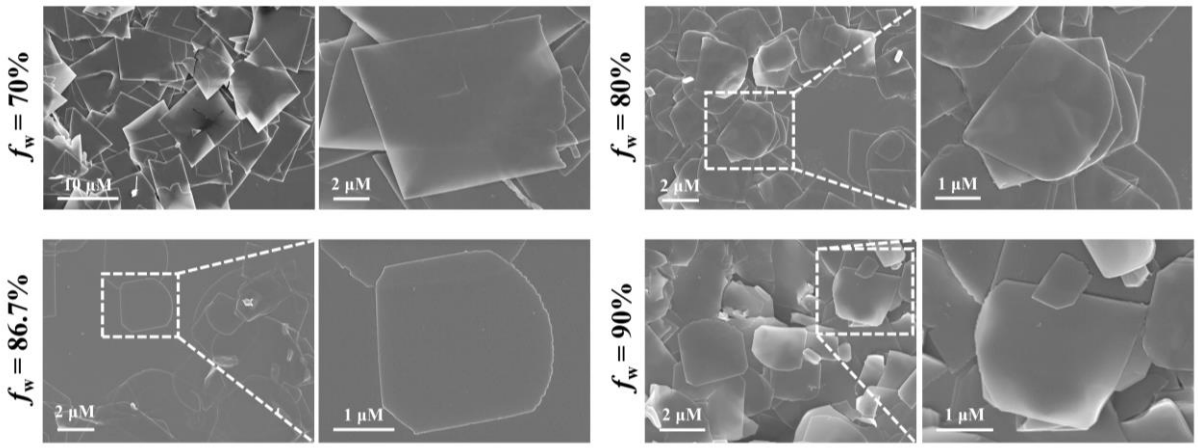

Fig. S2 SEM images of **1NS** in H_2O/CH_3CN with f_w of 70%, 80%, 86.7% and 90% at 50 μM, respectively.

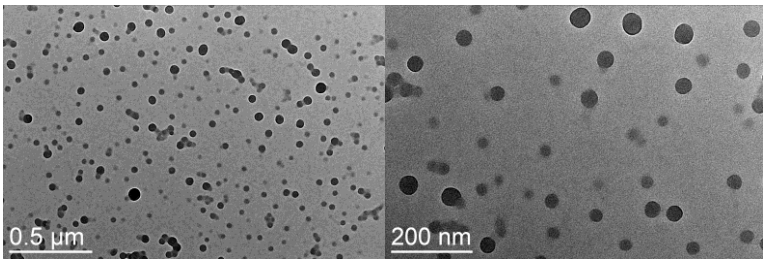

Fig. S3 TEM images of **1NP** in H_2O/CH_3CN with f_w of 90% at 50 μM.

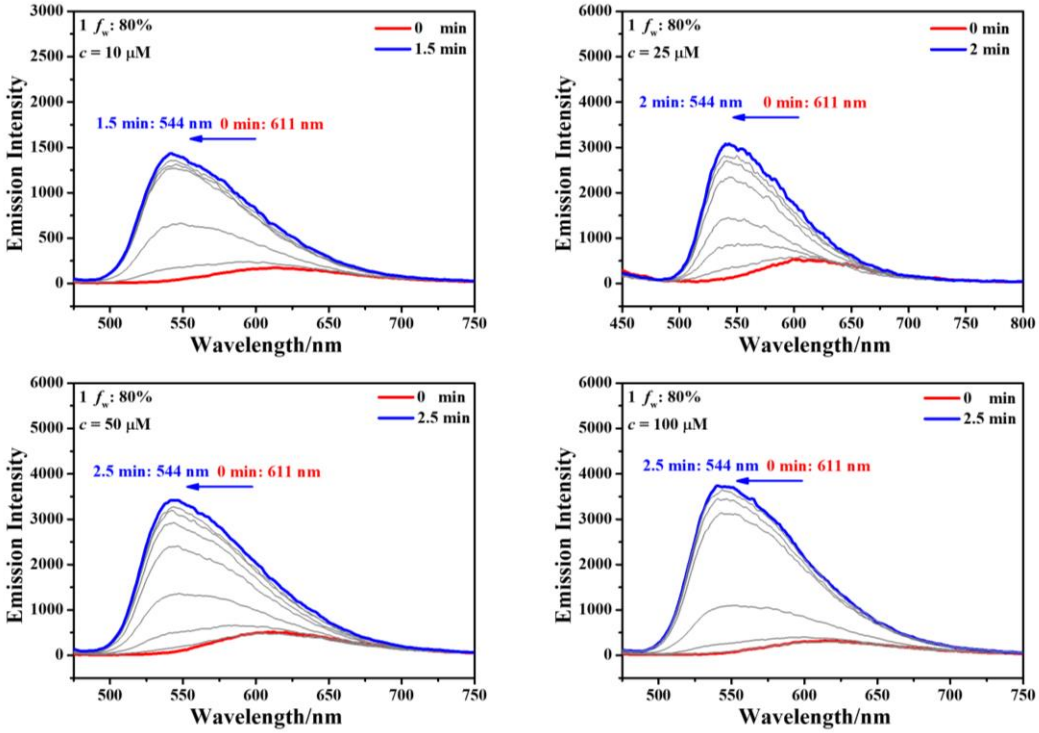

Fig. S4 Time-dependent emission spectra of **1** with f_w of 80% at different concentrations: 10 μM, 25 μM, 50 μM, and 100 μM, respectively, 298 K.

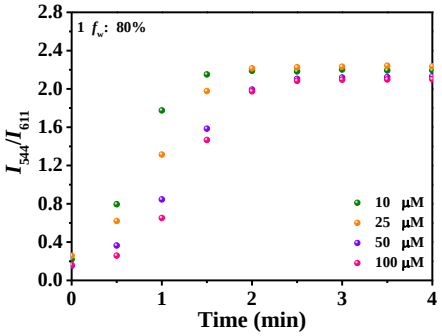

Fig. S5 Time-dependent relative emission intensity ratios of **1** (emission intensity at 544 nm/611 nm, I_{544}/I_{611}) at different initial concentrations with f_w of 80%, 298 K.

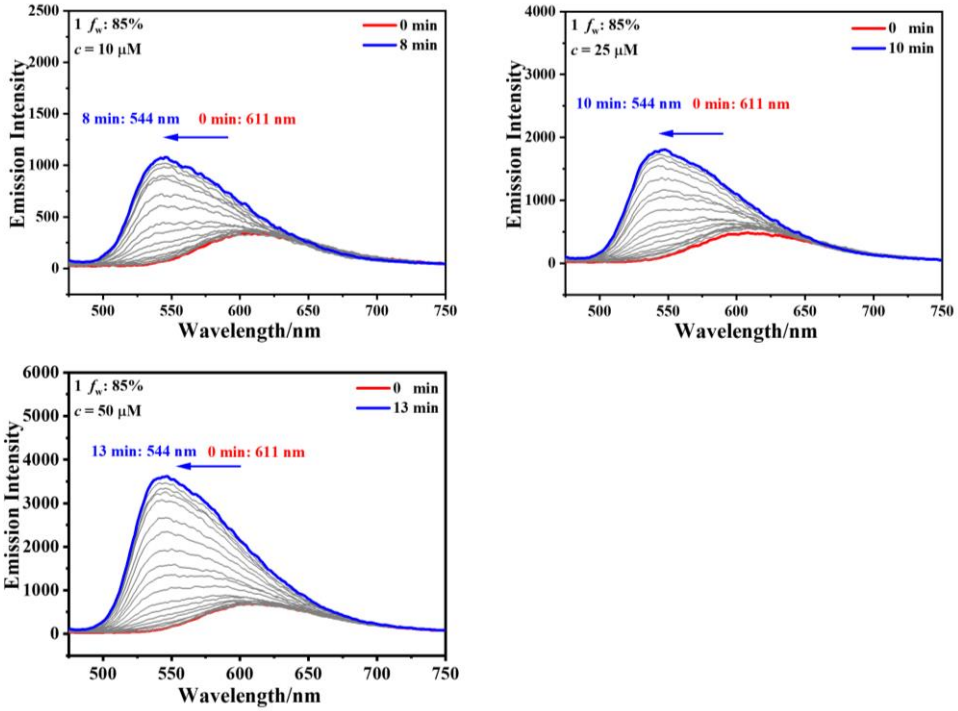

Fig. S6 Time-dependent emission spectra of **1** in H_2O/CH_3CN with f_w of 85% at different concentrations: 10 μM, 25 μM, and 50 μM, respectively, 298 K.

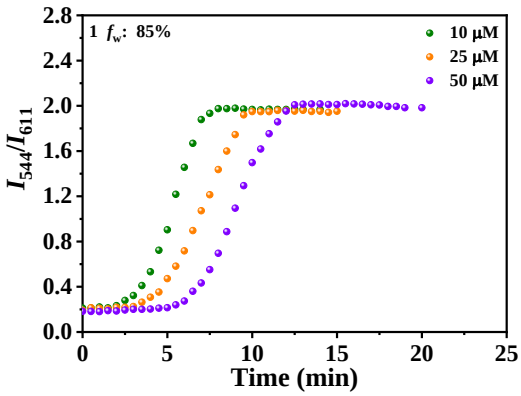

Fig. S7 Time-dependent relative emission intensity ratios of **1** (emission intensity at 544 nm/611 nm, I_{544}/I_{611}) at different initial concentrations with f_w of 85%, 298 K.

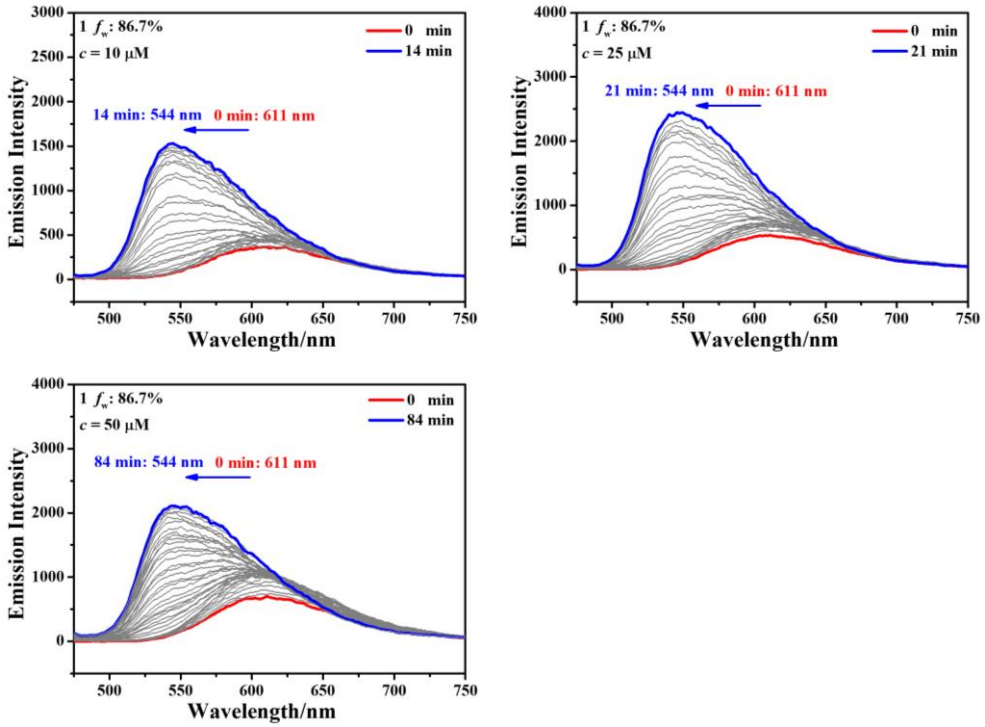

Fig. S8 Time-dependent emission spectra of **1** in H_2O/CH_3CN with f_w of 86.7% at different concentrations: 10 μM, 25 μM, and 50 μM, respectively, 298 K.

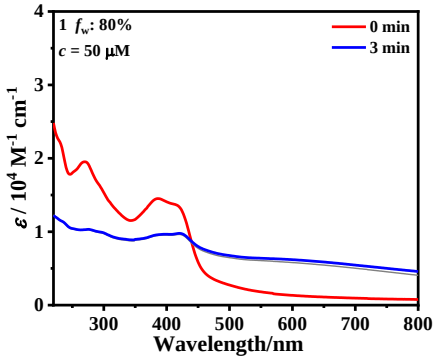

Fig. S9 Time-dependent UV-Vis spectra of **1** with f_w of 80% at 50 μM, 298 K.

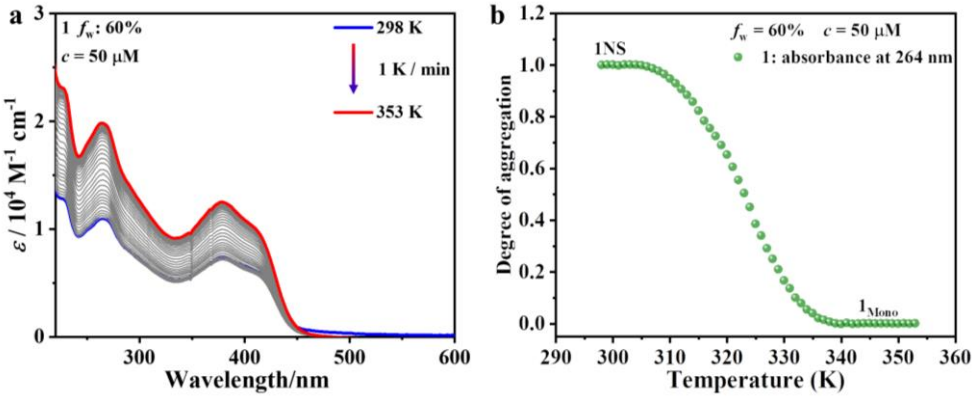

Fig. S10 Temperature-dependent UV-Vis absorption spectra of **1NS** at 60% water content (**a**, heating rate: 1 K/min, 50 μM) and the corresponding degree of aggregation curve of **1NS** (**b**, olive sphere).

Tab. S1 Thermodynamic parameters obtained by fitting the curves in **Fig. 2d** with the nucleation-elongation model (f_w = 60%).

Complex	ΔH^0 / kJ mol^{-1}	ΔS^0 / kJ mol^{-1} T^{-1}	ΔH^0_{nucl} / kJ mol^{-1}	T_e / K
1	-168.8	-0.45	-15.1	315.8

The experiments for living supramolecular polymerization

Seed preparation of 1NS$_{seed}$

1NS$_{seed}$ were prepared by applying ultrasound for 15 min to **1NP** in H_2O/CH_3CN (3.0 mL, 50 μM) with f_w of 86.7%.

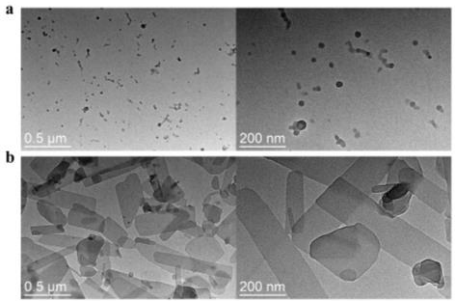

Fig. S11 TEM images of **1NP** (**a**) and **1NS$_{seed}$** (**b**), respectively.

The experiments for the results in Fig. 3b

1NS$_{seed}$ in H_2O/CH_3CN with f_w of 86.7% (30, 50, 75, 100 and 300 μL, respectively, 50 μM) were added to 3 mL of **1NP** in H_2O/CH_3CN with f_w of 86.7% (50 μM) at the 5th min, and the mixture was monitored by emission spectroscopy.

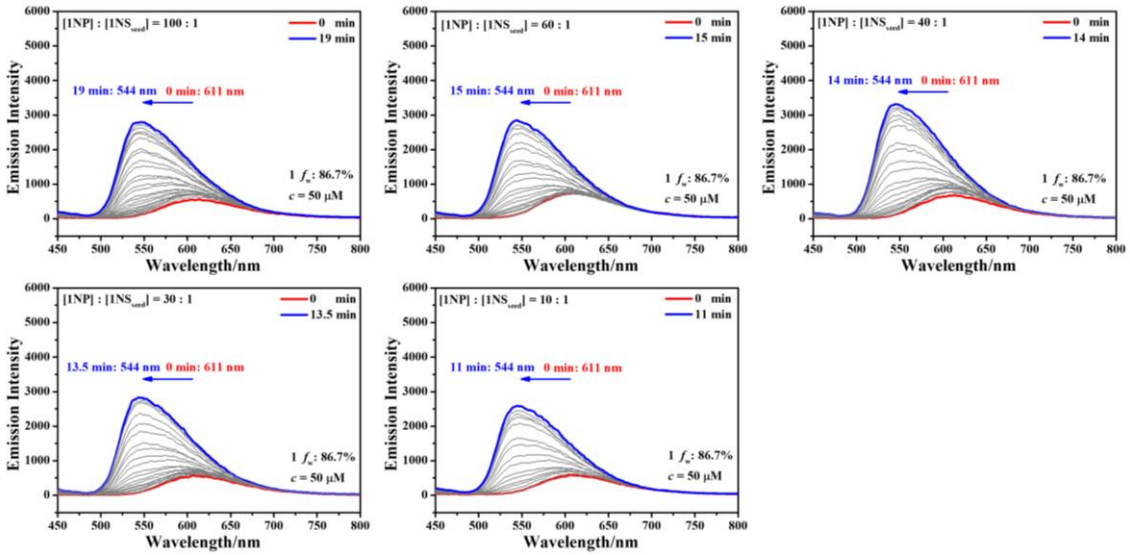

Fig. S12 Time-dependent emission spectra observed upon mixing **1NP** and **1NS$_{seed}$** under [**1NP**]/[**1NS$_{seed}$**] = 100:1, 60:1, 40:1, 30:1, and 10:1, respectively. The overall concentration of **1** is 50 μM, f_w: 86.7%, 298 K.

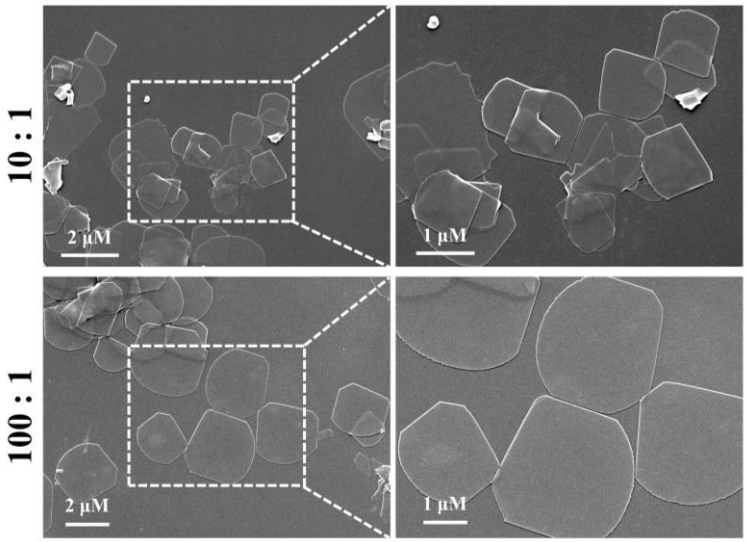

Fig. S13 SEM images of **1NS** obtained after the seeded polymerization with f_w of 86.7% under [**1NP**]/[**1NS**$_{seed}$] = 100:1 and 10:1, respectively. 50 μM, 298 K.

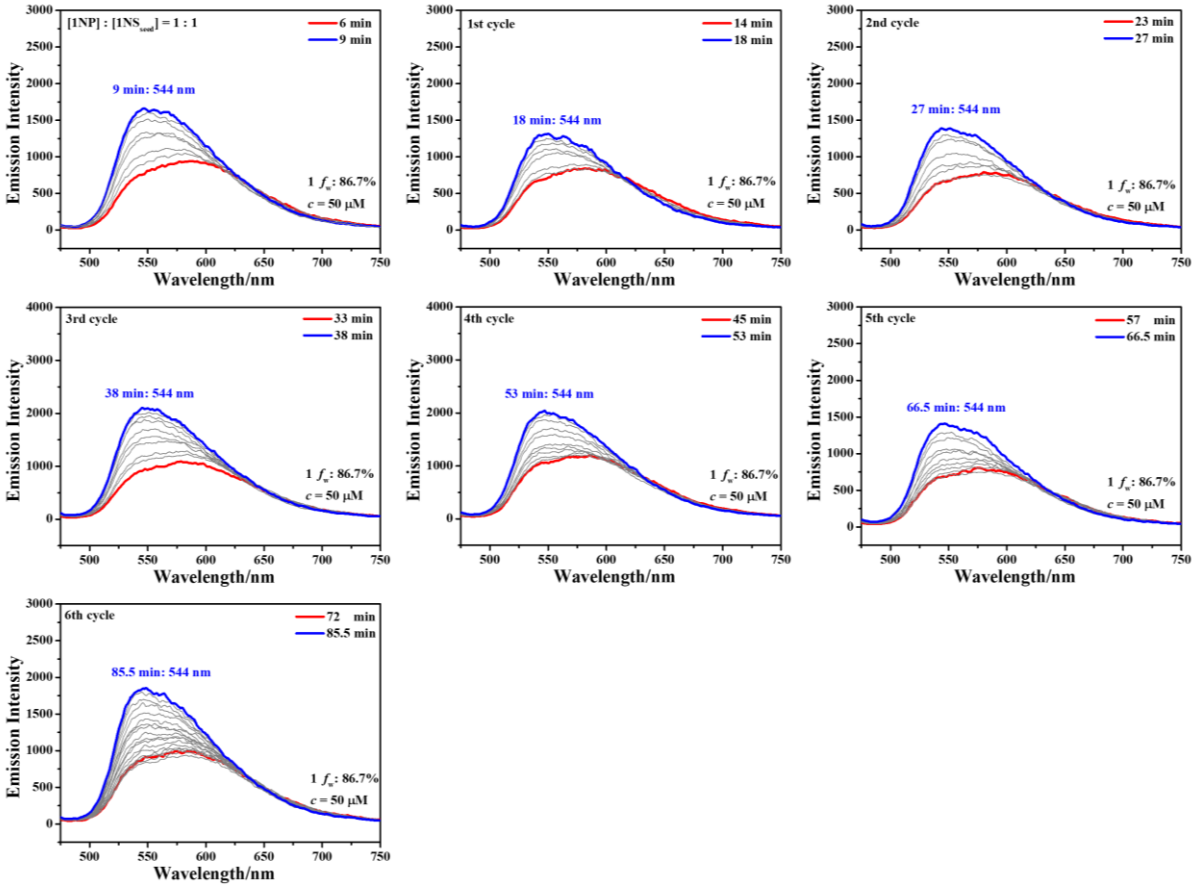

Fig. S14 Time-dependent emission spectra of living supramolecular polymerization cycles. The initial vol. ratio of [**1NP**]:[**1NS**$_{seed}$] = 1:1, the overall concentration of **1** is 50 μM, f_w: 86.7%, 298 K.

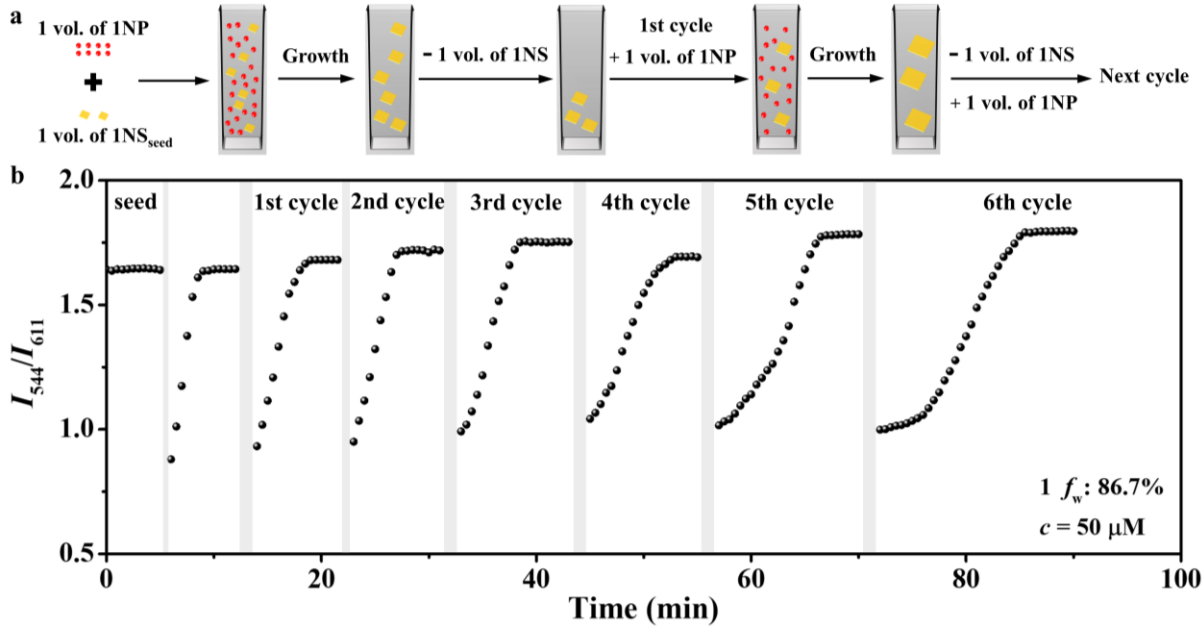

Fig. S15 (**a**) Schematic diagram of experimental operation process of living supramolecular polymerization cycles. (**b**) Time-dependent relative emission intensity ratios of **1** at I_{544}/I_{611} while **1NS$_{seed}$** was diluted with **1NP**, showing repeated polymerization on each addition of **1NP**, 298 K. During the time ranges highlighted in grey, the sample compartment was opened to remove 1 vol. of **1NS** suspension and add 1 vol. of **1NP** suspension (maintaining the f_w with 86.7% and the concentration at 50 μM).

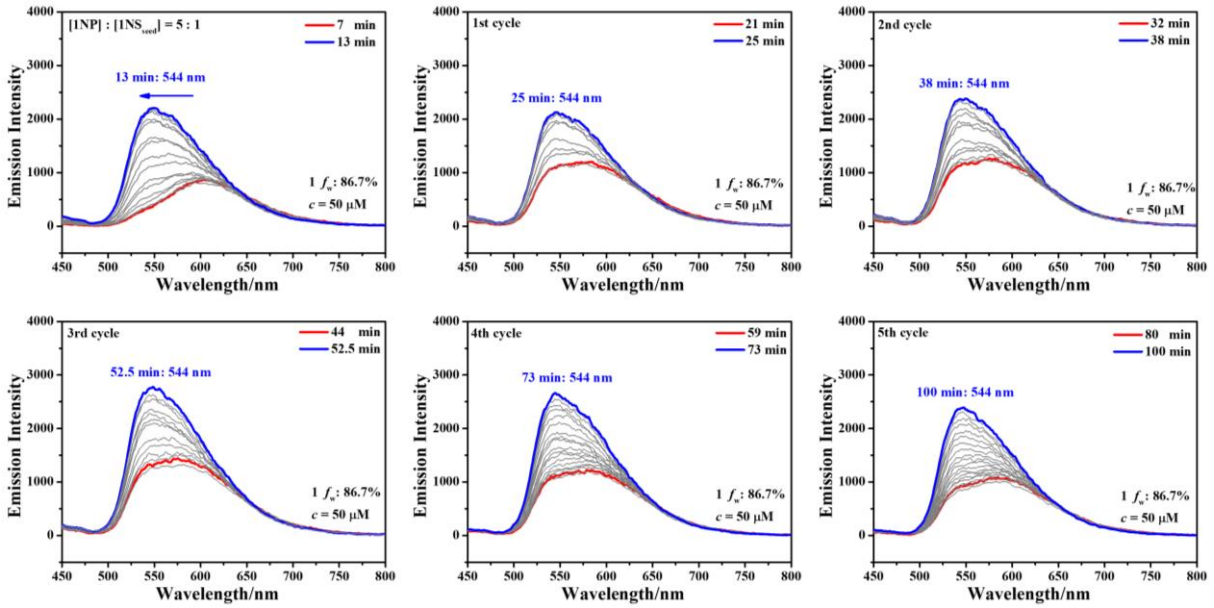

Fig. S16 Time-dependent emission spectra of living supramolecular polymerization cycles. The initial vol. ratio of [**1NP**]:[**1NS$_{seed}$**] = 5:1, the overall concentration of **1** is 50 μM, f_w: 86.7%, 298 K.

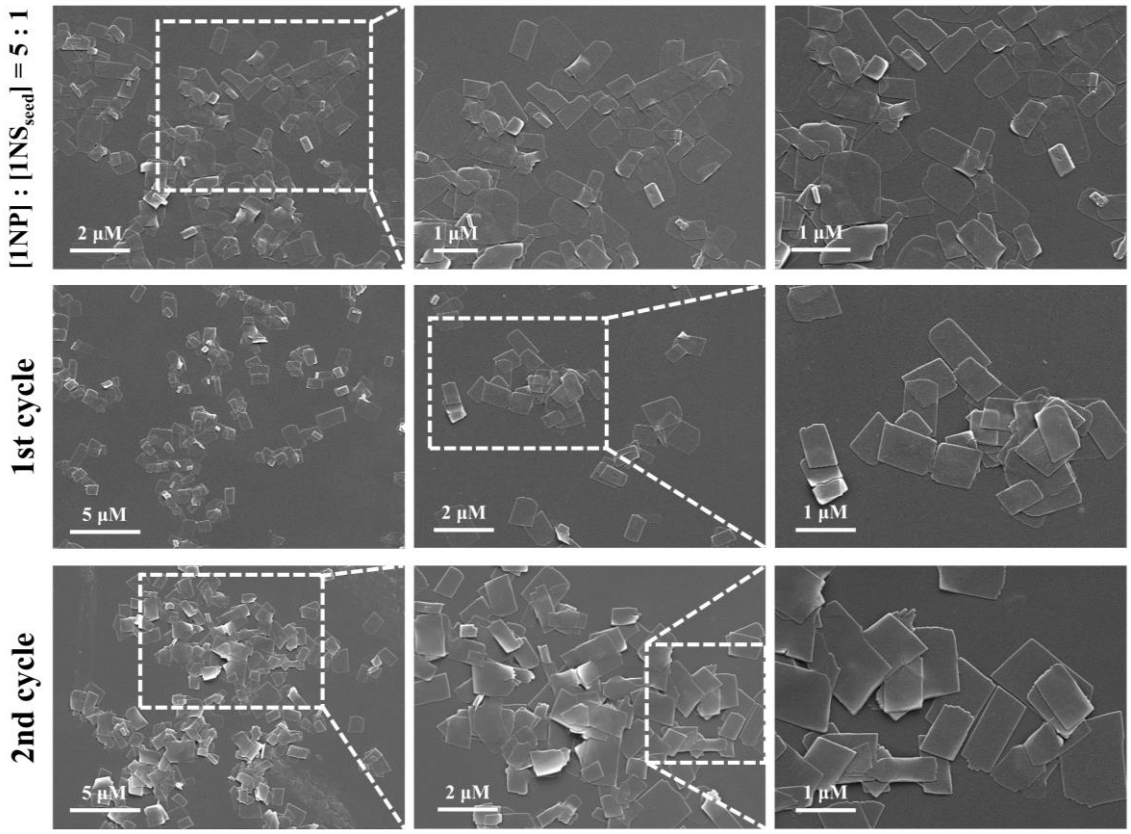

Fig. S17 SEM images of **1NS** obtained after each living supramolecular polymerization cycle with f_w of 86.7% at 50 μM, 298 K. The initial vol. ratio of [**1NP**]:[**1NS$_{seed}$**] = 5:1.

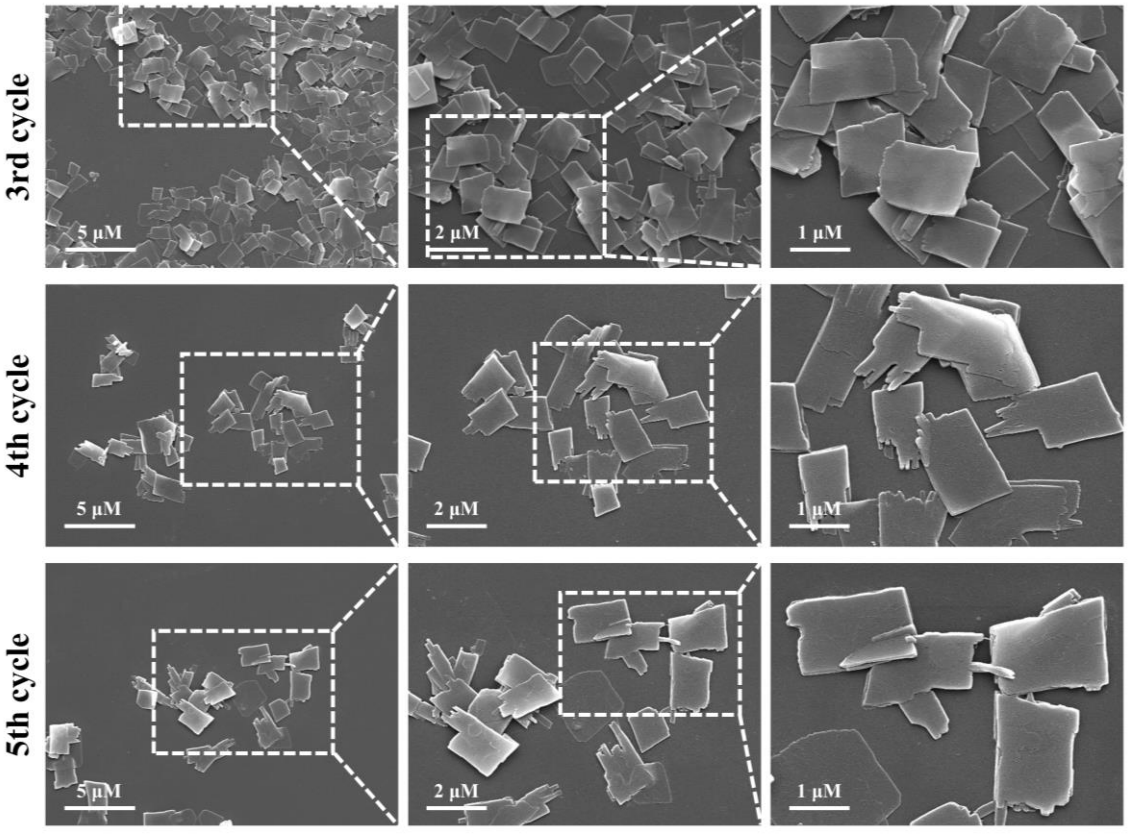

Fig. S18 SEM images of **1NS** obtained after each living supramolecular polymerization cycle with f_w of 86.7% at 50 μM, 298 K. The initial vol. ratio of [**1NP**]:[**1NS$_{seed}$**] = 5:1.

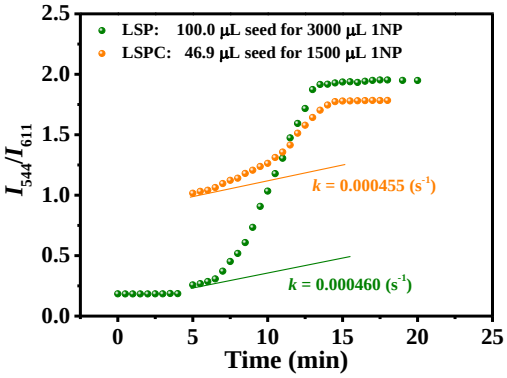

Fig. S19 Time-dependent I_{544}/I_{611} changes in the equivalent experimental groups, k represents the initial polymerization rate.

Self-assembly mode

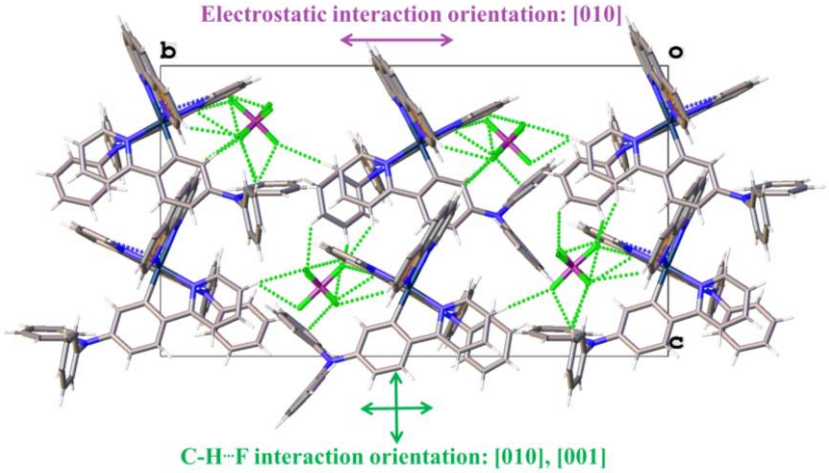

Fig. S20 Molecular stacking of **1** in the crystal state along the a-axis. The green dashed lines represent the C-H···F hydrogen bond. The orange planes represent the π-π planes. The black box represents the cell of **1**.

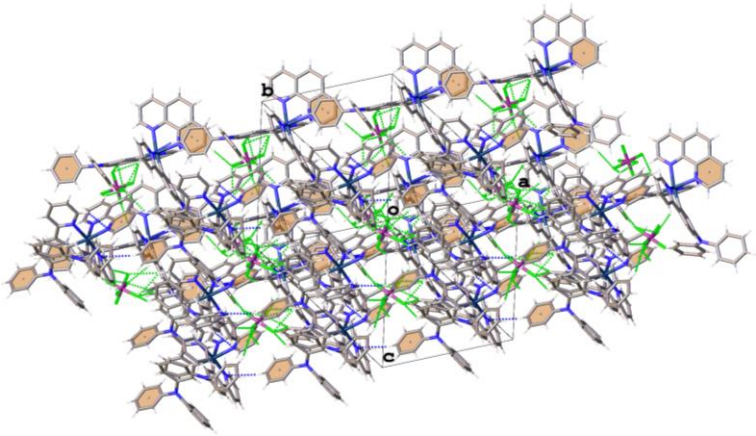

Fig. S21 Molecular stacking of **1** in the crystal state along the [111] direction. The green dashed lines represent the C-H···F hydrogen bond. The blue dashed lines represent the C-H···N hydrogen bond. The orange planes represent the π-π planes. The black box represents the cell of **1**.

Tab. S2 Crystal data of **1**.

Complex	**1**
Formula	$C_{58}H_{42}F_6IrN_6P$
Formula weight	1160.14
Crystal system	Monoclinic
Temperature	173.15
Space Group	Pn
Cell Lengths (Å)	a = 12.8519(2) b = 25.9976(5) c = 14.8768(3)
Cell Angles (°)	α = 90 β = 91.8810(10) γ = 90
Cell Volume (Å^3)	4967.94(16)
Z	4
Density (g/cm^3)	1.551
F(000)	2312.0
hmax, kmax, lmax	15, 32, 18
Absorption coefficient/mm^{-1}	6.083
R(int)	0.0845
Data/restraints/parameters	14221/20/1297
Goodness-of-fit on F^2	1.046
R_1[a] [$I > 2\sigma(I)$]	0.0486
wR_2[b] [$I > 2\sigma(I)$]	0.0965
R_1[a] (all data)	0.0604
wR_2[b] (all data)	0.1027
CCDC	1952377

$$^{[a]}R_1 = \sum||F_o| - |F_c|| / \sum|F_o|$$

$$^{[b]}wR_2 = [\sum w(F_o^2 - F_c^2)^2 / \sum w(F_o^2)^2]^{1/2}$$

Tab. S3 Centroid-centroid distances, angles and shift distances between π-π planes of **1**.

Centroid-centroid distances between π-π plane/Å	Mean distance/Å
3.98 3.96	3.97
Angles between π-π plane/°	Mean angle/°
13.21 5.80	9.51
Shift distances/Å	Mean distance/Å
1.34 1.78	1.56

Tab. S4 The distances and angles between the C-H···F and C-H···N hydrogen bonds in crystal of **1**.

Type	Atoms	Distances/Å	Angles/°
C-H···F (P_1)	C_{95}-H_{95}···F_3	2.62	167.1
	C_{39}-H_{39}···F_4	2.74	134.9
	C_{26}-H_{26}···F_3	2.76	156.2
	C_{50}-H_{50}···F_2	2.48	140.0
	C_{26}-H_{26}···F_1	2.71	131.6
	C_{11}-H_{11}···F_1	2.83	130.0
	C_{34}-H_{34}···F_5	2.93	139.0
	C_{39}-H_{39}···F_5	2.86	129.2
	C_{46}-H_{46}···F_5	2.76	123.2
	C_{39}-H_{39}···F_6	2.70	171.7
	C_{46}-H_{46}···F_6	2.46	170.3
	C_{16}-H_{16}···F_6	2.70	137.8
	C_{51}-H_{51}···F_6	2.92	137.4
C-H···F (P_2)	C_{14}-H_{14}···F_8	2.61	124.6
	C_{14}-H_{14}···F_9	2.56	162.7
	C_{74}-H_{74}···F_9	2.91	148.0
	C_{74}-H_{74}···F_{10}	2.87	132.2
	C_{107}-H_{107}···F_{10}	2.64	134.1
	C_{81}-H_{81}···F_{10}	2.57	122.7
	C_{81}-H_{81}···F_{11}	2.57	160.7
	C_{97}-H_{97}···F_{11}	2.94	121.0
	C_{90}-H_{90}···F_{11}	2.81	122.4
	C_{60}-H_{60}···F_{12}	2.69	133.2
	C_{68}-H_{68}···F_{10}	2.42	159.0
	C_{68}-H_{68}···F_{12}	2.42	136.3
	C_{91}-H_{91}···F_7	2.63	132.4
C-H···N (Intermolecular)	C_{56}-H_{56}···N_3	2.86	146.7
	C_{85}-H_{85}···N_{11}	2.85	147.8
C-H···N (Intramolecular)	C_{36}-H_{36}···N_2	2.62	120.5

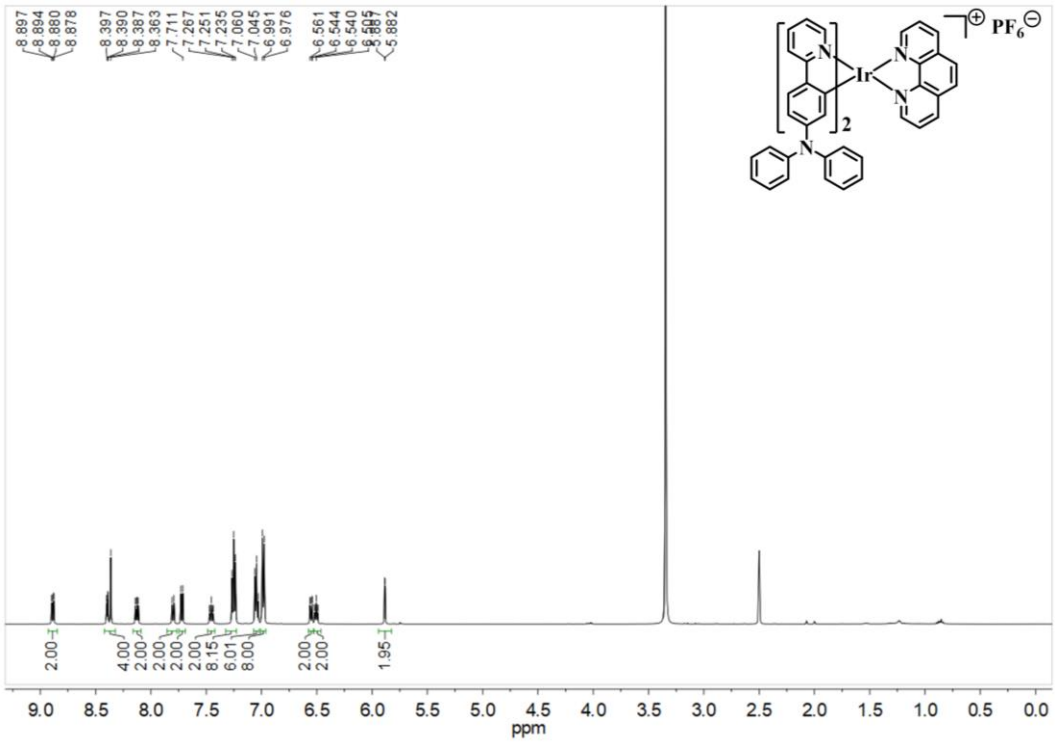

Fig. S22 ^{1}H NMR spectrum of **1** in DMSO-d_6.

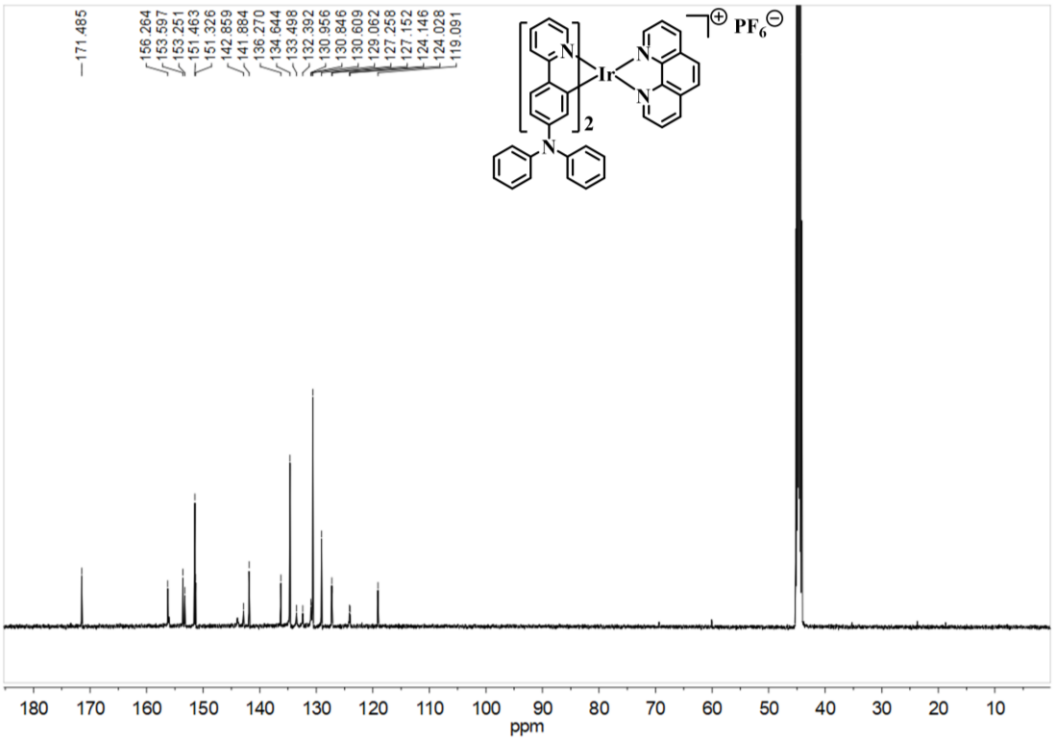

Fig. S23 ^{13}C NMR spectrum of **1** in DMSO-d_6.

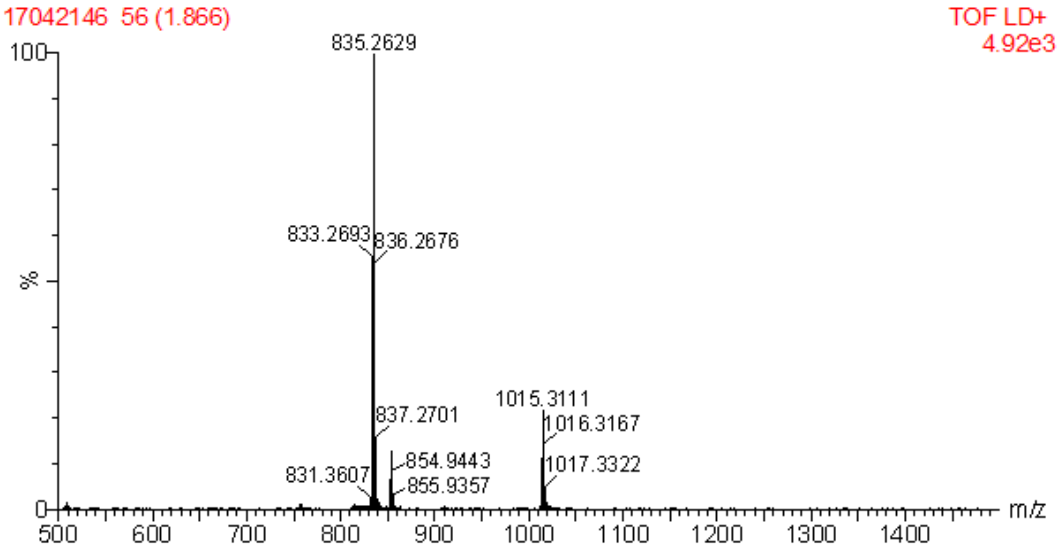

Fig. S24 The HRMS of **1**.

References

1. SMART, Data collection software v. version 5.629 (Bruker AXS Inc., Madison WI., 2003).
2. SAINT, Data reduction software v. version 6.45 (Bruker AXS Inc., Madison WI., 2003).
3. G. M. Sheldrick, Crystal structure refinement with SHELXL. *Acta Crystallogr. C Struct. Chem*., 2015, **71**, 3-8.
4. O. V. Dolomanov, L. J. Bourhis, R. J. Gildea, J. A. K. Howard and H. Puschmann, OLEX2: a complete structure solution, refinement and analysis program. *J. Appl. Crystallogr*., 2009, **42**, 339-341.